Suppression of small scale dynamo action by an imposed magnetic field

Nils Erland L. Haugen

Department of Physics, The Norwegian University of Science and Technology, Høyskoleringen 5, N-7034 Trondheim, Norway*

Axel Brandenburg NORDITA, Blegdamsvej 17, DK-2100 Copenhagen Ø, Denmar k^{\dagger} (Dated: November 14, 2018, Revision: 1.98)

Non-helical hydromagnetic turbulence with an externally imposed magnetic field is investigated using direct numerical simulations. It is shown that the imposed magnetic field lowers the spectral magnetic energy in the inertial range. This is explained by a suppression of the small scale dynamo. At large scales, however, the spectral magnetic energy increases with increasing imposed field strength for moderately strong fields, and decreases only slightly for even stronger fields. The presence of Alfvén waves is explicitly confirmed by monitoring the evolution of magnetic field and velocity at one point. The frequency ω agrees with $v_A k_1$, where v_A is the Alfvén speed and k_1 is the smallest wavenumber in the box.

I. INTRODUCTION

Turbulent magnetic fields are seen in many astrophysical settings [1, 2, 3]. Such magnetic fields usually result from the conversion of kinetic energy into magnetic energy, i.e. from dynamo action. Numerical simulations show that a dynamo-generated magnetic field can be of appreciable strength even when there is no kinetic helicity [4, 5]. Simulations have recently also shown that at scales smaller than about five times the energy carrying scale the magnetic energy spectrum seems to enter an inertial subrange where the magnetic spectral energy exceeds the kinetic spectral energy [6]. This means that over any subvolume, whose scale is within the inertial range, there is always a larger scale component of the field with significant strength. This raises the question whether one can model the small scale properties of such turbulence simply by imposing a magnetic field.

A lot of work has already been devoted to studying hydromagnetic turbulence in the presence of an external field [7, 8, 9]. Nevertheless, the super-equipartition magnetic energy seen in simulations without imposed field has never been seen in simulations with imposed field. An exception is when the magnetic Prandtl number is large[10]. However, the super-equipartition is then seen between the viscous and the resistive cutoff - not in the inertial range. It is one of our goals to elucidate this puzzle. Likewise, although dynamos with helicity can produce substantial super-equipartition on the scale of the system, they too are not able to produce superequipartition in the inertial range [11]. In that sense the difference between dynamos with and without imposed field is similar to the difference between helical and nonhelical dynamos.

The views on the effects of external fields are divided. A common scenario that applies when the conditions for

dynamo action are not met (e.g. if the magnetic Reynolds number is too small), is one where a local magnetic field can be enhanced simply by winding up an external magnetic field. Possible candidates where this may be the case are Io and Ganymede, in which convection interacts with the field of Jupiter leading to local field enhancement [12, 13, 14]. A similar possibility may also apply to the solar convection zone where the large scale field of the 11 year solar cycle is primarily located at the bottom of the convection zone [15], but the overlying convection zone may shred the field to produce small scale field [16]. Another possibility that has been discussed more recently is that the small scale field at the solar surface could be generated locally by a small scale dynamo operating near the surface [17].

In hydromagnetic turbulence theory magnetic and kinetic energy are assumed to cascade from large to small scales, similar to the hydrodynamic case, although recent work has established a strong intrinsic anisotropy [18], which has no counterpart in the hydrodynamic case. However, this theory does not address the possibility of dynamo action. It remains therefore an open question as to what is the nature of the interaction resulting from imposed and dynamo-generated magnetic fields. In particular, we shall present evidence that the imposed magnetic field does not enhance dynamo action. Instead, the external field does actually suppress dynamo action, albeit in a subtle way because the rms turbulent velocity is generally *not* decreased by a modestly strong magnetic field. We show that the suppression can be associated with the work term resulting from the Lorentz force due to the imposed field. It turns out that this term changes sign above a certain field strength such that a certain fraction of magnetic energy flows backwards to enhance the kinetic energy instead.

II. EQUATIONS

We adopt an isothermal equation of state with constant (isothermal) sound speed c_s , so the pressure p is

TABLE I: Summary of the different runs with forcing at $k_{\rm f}=1.5$. All runs have magnetic Prandtl number unity. The field strengths 0.06, 0.3, and 3.0 correspond roughly to 0.5, 2.0, and 20 times $B_{\rm eq}=\sqrt{\mu_0\rho_0}u_{\rm rms}$.

Run	Res.	$\nu = \eta$	Re_M	$b_{ m rms}$	$u_{ m rms}$	B_0
B4	128^{3}	4×10^{-4}	280	0.076	0.17	0.3
C1	256^{3}	2×10^{-4}	400	0.062	0.12	0
C2	256^{3}	2×10^{-4}	400	0.070	0.12	0.01
C3	256^{3}	2×10^{-4}	370	0.094	0.12	0.06
C4	256^{3}	2×10^{-4}	500	0.088	0.19	0.3
C5	256^{3}	2×10^{-4}	500	0.075	0.15	3
D4	512^{3}	1×10^{-4}	930	0.089	0.14	0.3
E1	1024^{3}	8×10^{-5}	1000	0.075	0.12	0

related to the density ρ by $p = \rho c_s^2$. The equation of motion is written in the form

$$\frac{\mathrm{D}\boldsymbol{u}}{\mathrm{D}t} = -c_{\mathrm{s}}^{2} \nabla \ln \rho + \frac{\boldsymbol{J} \times \boldsymbol{B}}{\rho} + \boldsymbol{F}_{\mathrm{visc}} + \boldsymbol{f}, \qquad (1)$$

where $D/Dt = \partial/\partial t + \boldsymbol{u} \cdot \boldsymbol{\nabla}$ is the advective derivative, $\boldsymbol{J} = \boldsymbol{\nabla} \times \boldsymbol{B}/\mu_0$ is the current density, μ_0 is the vacuum permeability,

$$F_{\text{visc}} = \nu \left(\nabla^2 \boldsymbol{u} + \frac{1}{3} \boldsymbol{\nabla} \boldsymbol{\nabla} \cdot \boldsymbol{u} + 2 \boldsymbol{S} \cdot \boldsymbol{\nabla} \ln \rho \right), \quad (2)$$

is the viscous force, $\nu = \text{const}$ is the kinematic viscosity,

$$S_{ij} = \frac{1}{2} \left(\frac{\partial u_i}{\partial x_j} + \frac{\partial u_j}{\partial x_i} - \frac{2}{3} \delta_{ij} \nabla \cdot \boldsymbol{u} \right)$$
 (3)

is the traceless rate of strain tensor, and \boldsymbol{f} is a random forcing function that consists of non-helical plane waves; see Refs [6, 19] for details. The continuity equation is written in terms of the logarithmic density,

$$\frac{\mathrm{D}\ln\rho}{\mathrm{D}t} = -\boldsymbol{\nabla}\cdot\boldsymbol{u},\tag{4}$$

and the induction equation is solved in terms of the magnetic vector potential \mathbf{A} ,

$$\frac{\partial \mathbf{A}}{\partial t} = \mathbf{u} \times \mathbf{B} + \eta \nabla^2 \mathbf{A},\tag{5}$$

where $\eta = \text{const}$ is the magnetic diffusivity, and $\boldsymbol{B} = \boldsymbol{B}_0 + \boldsymbol{b}$ is the magnetic field consisting of the imposed uniform (k=0) field, \boldsymbol{B}_0 , and the deviations from the imposed field $\boldsymbol{b} = \nabla \times \boldsymbol{A}$. This split is necessary because the vector potential corresponding to \boldsymbol{B}_0 cannot be periodic, while both \boldsymbol{B} and \boldsymbol{A} can well be assumed to be periodic.

In the simulations summarized in Table I we have used the same method as described in Ref. [19]. Kinetic and magnetic Reynolds numbers are defined as

$$\operatorname{Re} = \frac{u_{\mathrm{rms}}}{\nu k_{\mathrm{f}}}, \quad \operatorname{Re}_{\mathrm{M}} = \frac{u_{\mathrm{rms}}}{\eta k_{\mathrm{f}}},$$
 (6)

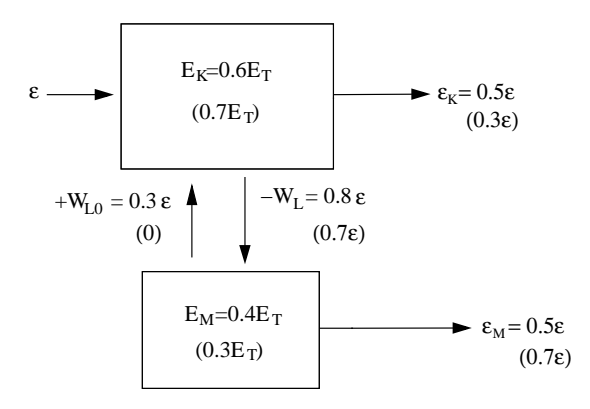


FIG. 1: Sketch of the energy budget showing the kinetic and magnetic energy reservoirs together with the flow of energy for Run D4. The numbers in parentheses correspond to Run E1 without an imposed field. The total dissipation rate is denoted by $\epsilon \equiv \epsilon_{\rm K} + \epsilon_{\rm M}$, which is the sum of kinetic and magnetic energy dissipation rates. The + sign on $W_{\rm L0}$ and the direction of the corresponding arrow emphasize that, at least for sufficiently strong imposed fields, energy flows from the magnetic to the kinetic energy reservoir.

respectively. Here, $k_{\rm f}$ is the average forcing wavenumber and ${\rm Pr_M} = \nu/\eta \equiv {\rm Re_M/Re}$ is the magnetic Prandtl number. In all cases studied below we assume ${\rm Pr_M} = 1$. We study cases where $k_{\rm f}$ is either 1.5 or 5.

The Pencil Code [20] is used for all our simulations. The resolution is varied between 128^3 and 1024^3 meshpoints. Although we solve the compressible equations, the sound speed is large compared with the turbulent velocities. We find that the energies of solenoidal and potential components of the flow have a ratio $E_{\rm pot}/E_{\rm sol}\approx 10^{-4}\text{--}10^{-2}$ for most scales; only towards the Nyquist frequency the ratio increases to about 0.1. Thus, our results should be close to the incompressible limit.

We use non-dimensional quantities by measuring length in units of $1/k_1$ (where $k_1 = 2\pi/L$ is the smallest wavenumber in the box of size L; in the present case $L = 2\pi$), speed in units of the isothermal sound speed c_s , density in units of the initial value ρ_0 , and magnetic field in units of $(\mu_0 \rho_0 c_s^2)^{1/2}$.

III. ENERGY BALANCE

A sketch of the overall energy budget is given in Fig. 1 where we show the magnetic and kinetic energy reservoirs together with arrows indicating the flow of energy. The arrow pointing into the kinetic energy reservoir is the energy flux ϵ entering the simulation through the external forcing, while the arrows pointing to the right from the kinetic and magnetic energy reservoirs denote viscous and Joule dissipation, i.e. $\epsilon_{\rm K}$ and $\epsilon_{\rm M}$, respectively. On the average and in the statistically steady state we expect $\epsilon = \epsilon_{\rm K} + \epsilon_{\rm M}$.

The two arrows between the kinetic and magnetic energy reservoirs correspond to the contributions to the

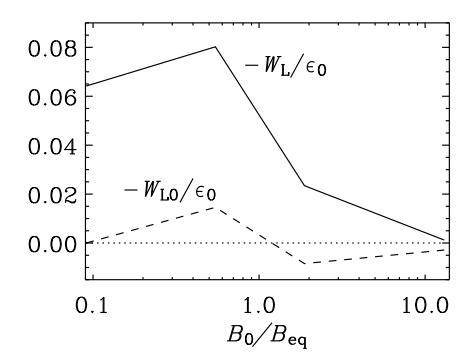


FIG. 2: Dependence of $-W_{\rm L}$ (solid line) and $-W_{\rm L0}$ (dashed line) on the imposed field strength, B_0 . Here $B_{\rm eq} = \sqrt{\mu_0 \rho_0} u_{\rm rms}$ is the equipartition field strength and $\epsilon_0 = k_{\rm f} \rho_0 u_{\rm rms}^3$ is a reference value for the energy flux. $k_{\rm f} = 1.5$.

work done against the Lorentz force. In general this work term can be written as $\langle \boldsymbol{u}\cdot(\boldsymbol{j}\times\boldsymbol{B})\rangle$, where we have used $\boldsymbol{j}=\boldsymbol{J}$ to emphasize that the current density has vanishing volume average. However, since $\boldsymbol{B}=\boldsymbol{B}_0+\boldsymbol{b}$, where $\boldsymbol{b}=\boldsymbol{\nabla}\times\boldsymbol{A}$ is the departure from the imposed field (also with vanishing volume average), we can divide the work term into a contribution from the fluctuating field, $\langle \boldsymbol{u}\cdot(\boldsymbol{j}\times\boldsymbol{b})\rangle$, and one from the imposed field, $\langle \boldsymbol{u}\cdot(\boldsymbol{j}\times\boldsymbol{B}_0)\rangle$. The latter can also be written as $\boldsymbol{B}_0\cdot\langle\boldsymbol{u}\times\boldsymbol{j}\rangle$, which emphasizes the fact that this term is quadratic in the fluctuations and can hence only transfer energy between kinetic and magnetic energy reservoirs at the same wavenumber. We can thus write

$$\frac{\mathrm{d}E_{\mathrm{M}}}{\mathrm{d}t} = -W_{\mathrm{L}} - W_{\mathrm{L}0} - \epsilon_{\mathrm{M}},\tag{7}$$

where $E_{\rm M} = \langle \boldsymbol{b}^2 \rangle / \mu_0$ is the magnetic energy (per unit volume) of the induced field without the imposed field, $W_{\rm L} = \langle \boldsymbol{u} \cdot (\boldsymbol{j} \times \boldsymbol{b}) \rangle$ is the work done by the fluctuating fields, $W_{\rm L0} = \boldsymbol{B}_0 \cdot \langle \boldsymbol{u} \times \boldsymbol{j} \rangle$ is the work done against winding up the imposed mean field, and $\epsilon_{\rm M} = \eta \mu_0 \langle \boldsymbol{j}^2 \rangle$ is the loss from Joule heating. In a closed or periodic system such as the one considered here, there are no surface terms, which is why there is no term associated with the Poynting flux in Eq. (7).

The numbers on the arrows give the energy fluxes for a simulation with a moderately strong imposed field (Run D4). The numbers in parentheses are the corresponding values for a simulation without imposed fields. By comparing the two we see that with an imposed field the content of the magnetic energy reservoir is slightly increased. Nevertheless, magnetic dissipation has decreased and kinetic dissipation has increased. This suggests that an imposed magnetic field quenches the dynamo.

Naively one might have expected that the $-W_{L0}$ term always "helps" the dynamo and that it therefore always transfers energy from kinetic to magnetic energy by winding up the imposed field. This is however not

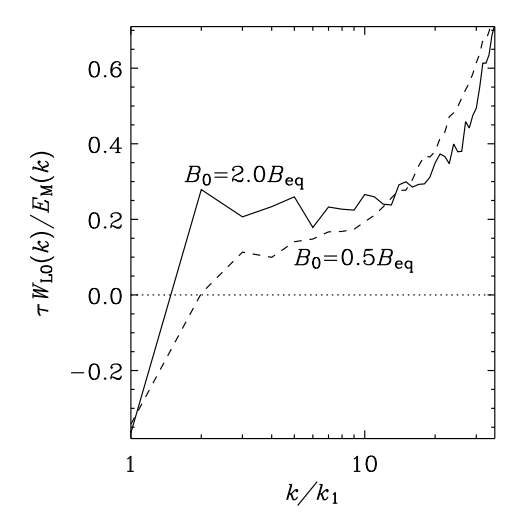


FIG. 3: Contribution to the spectral energy transfer between kinetic and magnetic energies due to the imposed field. Power spectrum of $\mathbf{B}_0 \cdot \langle \mathbf{u}_k \times \mathbf{j}_k \rangle$ normalized by E_k^M for run C4 (solid line) and run C3 (dashed line). We clearly see that at the box scale there is transport of energy from kinetic to magnetic field, while at all other scales the transport is in the opposite direction, i.e. there is a suppression of the magnetic field. It is also clear that the suppression is much stronger at the smallest scales.

the case. In Fig. 2 we show $W_{\rm L}$ and $W_{\rm L0}$, normalized by $\epsilon_0 = k_{\rm f} \rho_0 u_{\rm rms}^3$, as functions of imposed field strength. (In those units the total energy input to the system is $\epsilon \approx 0.07 \epsilon_0$.) The negative contribution from $-W_{\rm L0}$ for large field strengths is actually the main reason that simulations with strong imposed fields have less magnetic energy; see Table I. Since the $W_{\rm L0}$ term is local in k-space it also explains the general increase in kinetic energy at all scales.

To quantify the above statement, we discuss now the spectral energy transfer function, $W_{L0}(k) = \mathbf{B}_0 \cdot \langle \mathbf{u}_k \times \mathbf{j}_k \rangle$, where \mathbf{u}_k and \mathbf{j}_k are Fourier filtered velocity and current density. In Fig. 3 we plot the ratio of $W_{L0}(k)$ to the magnetic energy spectrum $E_{\mathrm{M}}(k)$, divided by the eddy turnover time $\tau = (k_{\mathrm{f}}u_{\mathrm{rms}})^{-1}$, using data from Runs C3 and C4. Here, the spectra are normalized such that $\int W_{L0}(k) \, \mathrm{d}k = W_{L0}$ and $\int E_{\mathrm{M}}(k) \, \mathrm{d}k = E_{\mathrm{M}}$. It turns out that, first, $W_{L0}(k)$ has a positive contribution to the magnetic energy at small wavenumbers. This explains the increase in magnetic energy at large scales (small wavenumbers). Second, at moderate and large wavenumbers, $W_{L0}(k)$ is positive, which explains the suppression of the magnetic energy.

IV. SPECTRAL ENERGY CHANGES

Next we investigate the effect of varying the strength of the imposed field on the magnetic and kinetic energies

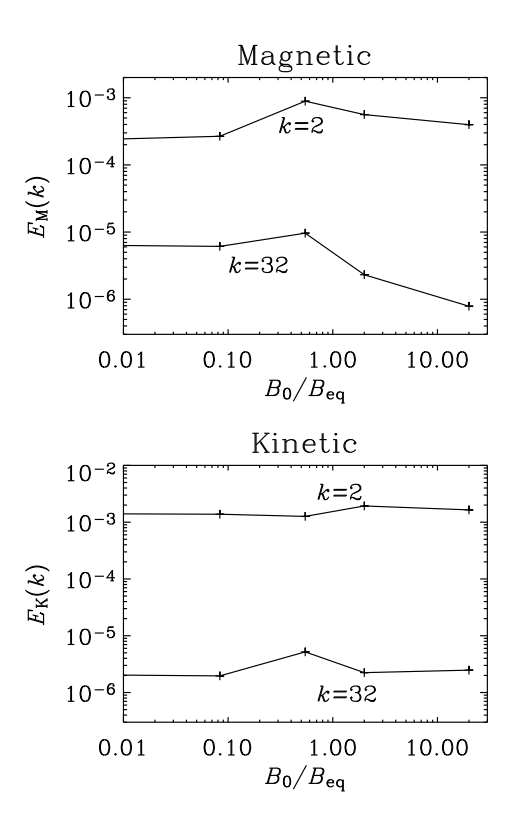


FIG. 4: Magnetic (top) and kinetic (bottom) spectral energy at wavenumbers 2 and 32 as a function of B_0 . $k_f = 1.5$.

at different wavenumbers; see Fig. 4. We see that around $B_0 \approx B_{\rm eq}$ the magnetic energy is somewhat enhanced at small wavenumbers (k=2, corresponding to modestly large scales), but decreased at large wavenumbers (k=32, corresponding to small scales). At the same time the effect on the velocity field is weak, but there is generally a tendency for enhanced velocities, especially at large scales.

When the forcing is at $k_{\rm f}=5$, instead of at $k_{\rm f}=1.5$, the trends are very similar as in Fig. 4; see Fig. 5. In particular, at large scales there is first an increase and then a decrease of the magnetic energy as the imposed field strength is increased, while for small scales the magnetic energy decreases for all imposed field strengths. We therefore conclude that the suppression of the magnetic field is, at least qualitatively, independent of the forcing scale.

The situation is different in the presence of helicity where it has been argued that it is particularly the large scale magnetic field at $k=k_1$ that is affected by the introduction of an imposed magnetic field [21]. This can be interpreted as a suppression of the α effect. Repeating the simulations of Ref. [21], we were able to confirm their findings; see also Ref. [22]. We also find that kinetic and magnetic energy spectra fall almost on top of each other when $B_0=2B_{\rm eq}$. This is just like in the case without imposed field [11], except at $k=k_1$ where there is an additional field component due to the α effect. Further-

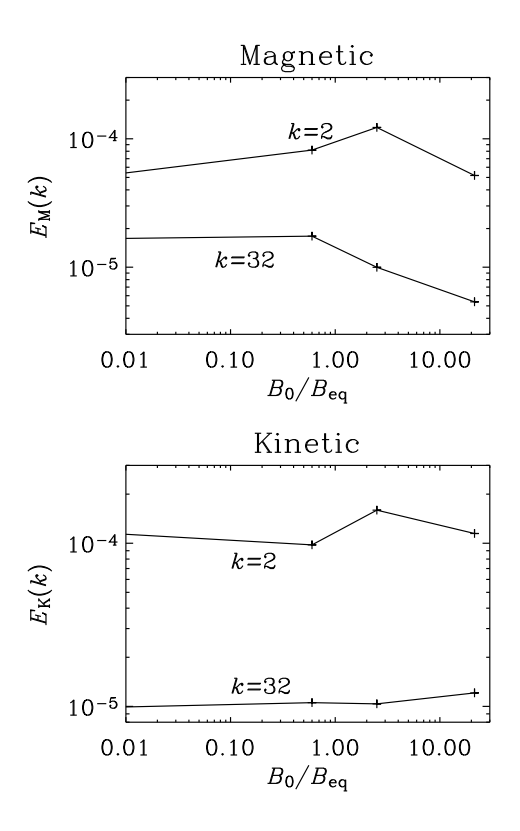


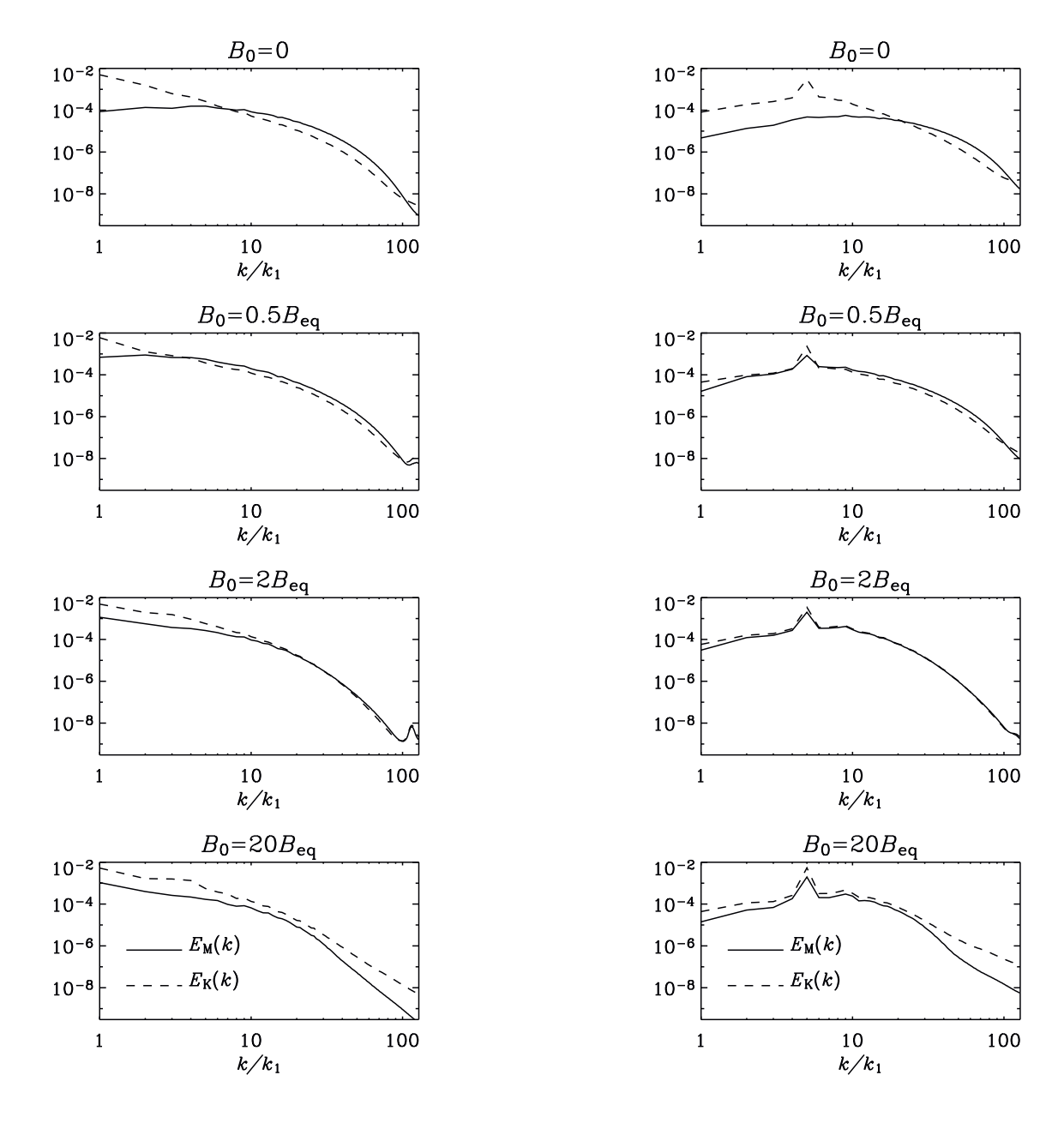
FIG. 5: Same as Fig. 4 but with forcing at $k_f = 5$.

more, increasing the field to $B_0 = 20 B_{\rm eq}$ we do recover the same suppression of the dynamo as without helicity, i.e. the spectra look similar to those of Run C5. Thus, the suppression of dynamo activity by the imposed field is rather general and affects equally helical and nonhelical dynamos.

It is generally believed that hydromagnetic turbulence can be described as an ensemble of Alfvén waves. This is true both for the Goldreich-Sridhar [18] and Iroshnikov-Kraichnan [23, 24] theories. This would then suggest that magnetic and kinetic energies should be comparable to one another at each scale. From Figs. 6 and 7 we see that magnetic and kinetic energies are close to each other, but generally not equal. This is also seen in the simulations of Cho & Vishniac [7]. Only when the imposed field is approximately equal in strength to the rms field do we have approximate equipartition between magnetic and kinetic energies at small scales.

V. SHAPE OF THE ENERGY SPECTRA

As the resolution is increased, one begins to see indications of the build-up of a short $k^{-5/3}$ inertial range of kinetic and magnetic energies at intermediate wavenumbers; see Fig. 8. The inertial range is as yet too short to be conclusive, and we therefore need larger simulations in order to be sure whether we have a real $k^{-5/3}$ slope or not.



so

FIG. 6: Magnetic and kinetic energy spectra for runs with different imposed field strengths (Runs C1 and C3-C5). In all cases $B_{\rm eq}=0.12$ –0.15; see Table I.

FIG. 7: Magnetic and kinetic energy spectra for runs with different imposed field strengths and forcing at k=5.

From Fig. 8 we also see that in the range $k_1 < k < 10$ the magnetic energy spectrum seems to follow a k^{-1} slope. For comparison, in the case without an imposed field the spectral magnetic energy was actually increasing with k and followed approximately a $k^{1/3}$ slope [19] at small k. The k^{-1} spectrum for imposed fields can be motivated by dimensional arguments: assume that the magnetic energy spectrum is a function of the imposed field strength B_0 and the wavenumber k, and that the spectrum is given by the ansatz $E_{\rm M}(k) = C B_0^a k^b$, then, from dimensional arguments, one finds a = 2 and b = -1,

$$E_{\rm M}(k) = CB_0^2 k^{-1} \tag{8}$$

where C is a dimensionless constant. Such a spectrum is expected if there is a mean field [25], but it may generally also appear at the low wavenumber end of the inertial subrange [26], and indications of this spectrum have been seen in convective dynamo simulations [27]. It turns out, however, that the value of C (obtained from a fit) is different for different values of B_0 , casting doubt on the validity of the assumptions behind Eq. (8). We therefore discard this simple explanation of the large scale magnetic spectrum. Indeed in Fig. 7 we see that we get no

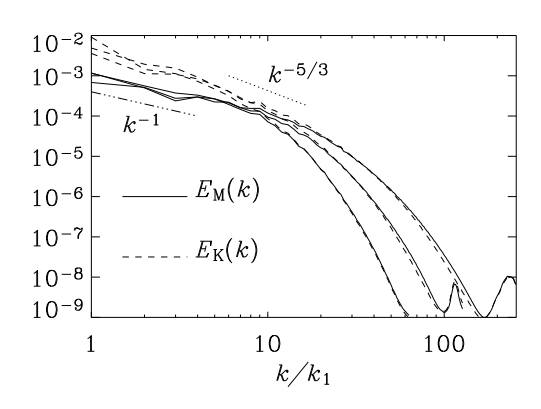


FIG. 8: Magnetic and kinetic power spectra for runs with $B_0 = 0.3$ (runs B4, C4 and D4).

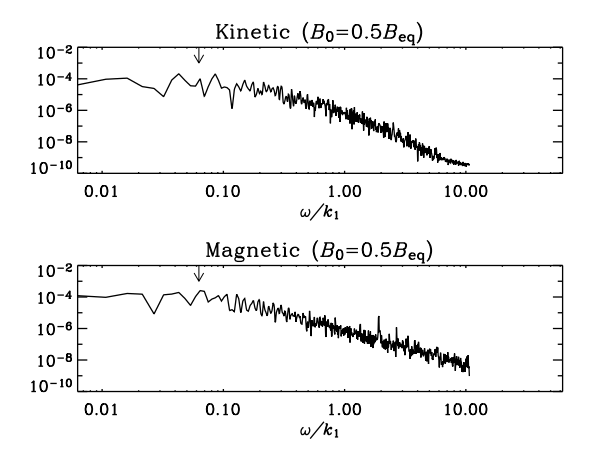


FIG. 9: Fourier spectra of time evolution of the magnetic and kinetic fields at one point in the box for simulation with $B_0=0.06$. The point of interest is chosen to be in the center of the box. The arrows represent the frequency of an Alfvén wave with a wavelength of the box size traveling along the imposed field. We clearly see that Alfvén waves are strongly present in the simulation.

longer a k^{-1} magnetic energy spectrum for large scales when the forcing is at k=5; instead the infrared part of the spectrum has an increasing slope close to $E_{\rm M}(k) \sim k$ for $k < k_{\rm f}$. Some intermediate behavior is seen when $k_{\rm f} = 2...3$; see Ref. [7] where no k^{-1} behavior was found.

VI. DIRECT EVIDENCE FOR ALFVÉN WAVES

Finally we look at the frequency power spectrum calculated from the time series of the magnetic field and velocity at one point in the simulation box; see Figs. 9 and 10. As expected, the larger the imposed magnetic field, the faster does the field oscillate. The peaks in the power spectra for $B_0 = 3.0$ and $B_0 = 0.06$ correspond to

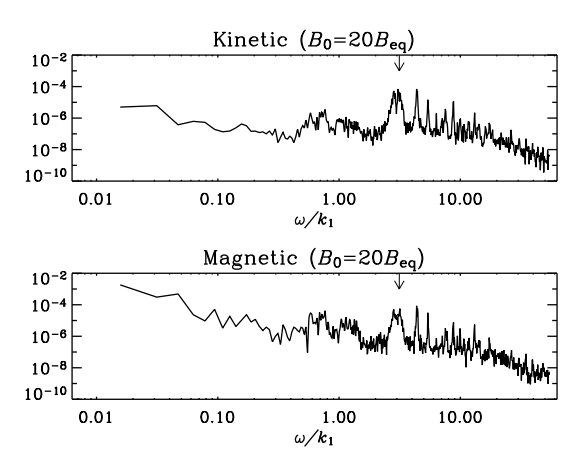


FIG. 10: Same as Fig. 9 but with $B_0 = 3.0$.

the frequency of the corresponding Alfvén wave,

$$\omega = v_{\rm A} k_1$$
, where $v_{\rm A} = B_0 / \sqrt{\mu_0 \rho_0}$ (9)

is the Alfvén speed. (In our case we have $\mu_0 = \rho_0 = 1$.) When B_0 is comparable to or less than $B_{\rm eq}$, the peaks in the spectra are no longer well pronounced.

For strong fields, however, the Alfvén peaks are seen quite clearly. It is conceivable that these Alfvén waves are stochastically excited by the turbulence. This might be similar to the stochastic driving of acoustic waves in the solar convection zone [28].

VII. CONCLUSION

The present studies have shown that a uniformly imposed magnetic field has two important effects on the magnetic field that is induced at finite wavenumbers $(k \neq 0)$. First, the magnetic field is slightly enhanced at and around the forcing wavenumber (corresponding to the energy carrying scale). Second, the magnetic field is quenched with increasing B_0 at all larger wavenumbers corresponding to the inertial and diffusive subranges.

The enhancement and suppression at the two different wavenumber ranges is associated with a corresponding wavenumber dependence of the work term, $B_0 \cdot \langle u \times j \rangle$. The suppression of the magnetic field in the inertial range is quite opposite to the behavior without imposed field when there is instead a significant enhancement of the magnetic energy spectrum over the kinetic energy spectrum. We therefore refer to this effect as a suppression of the dynamo by the imposed field.

The suppression of dynamo activity might be a consequence of the tendency toward two-dimensionalization of the turbulence by the large scale field [29]. Such an effect is well-known for low-Re_M hydromagnetic turbulence [30], and it is a mathematical theorem that there can be no dynamo action in two dimensions [31]. Of course, the turbulence does not really become two-dimensional, but instead the correlation length along the field becomes

large. This type of anisotropy is a crucial ingredient of the Goldreich-Sridhar theory [18].

The Goldreich-Sridhar theory also predicts that Alfven waves should be present in the system. This has been confirmed by inspecting velocities and magnetic fields at a single point in the middle of the simulation box. These Alfvén waves have the expected frequency $\omega_A = v_A k_1$. Furthermore, we do not find that there is equipartition between magnetic and kinetic energy spectra in the inertial range for large imposed field strengths. The absence of equipartition may be a consequence of the inertial range being still too short (or absent). In runs where $B_0 = B_{eq}$, on the other hand, there is clear evidence that kinetic and magnetic energy spectra fall on top of each other throughout the dissipation subrange. This is also in agreement with earlier results of Cho and collaborators [9], who considered the case where the imposed field had equipartition strength.

Whether or not models with imposed field can reproduce the situation in small sub-domains of simulations with no overall imposed field is still unclear. At first glance the answer seems to be no, because none of the simulations with imposed field have ever been able to produce super-equipartition in the inertial range, as it is seen in the nonhelical simulations without imposed field [6]. However, the reason for this may well lie in the still insufficient resolution of the simulations with no

imposed field – even though they do already have a resolution of 1024^3 meshpoints. It is indeed possible that, even though the kinetic and magnetic energy spectra are approximately parallel to each other over a certain range of wavenumbers and offset by a factor of about 2.5, they may actually converge at still larger wavenumbers. Preliminary indications of this have now been seen in simulations using hyperviscosity and hyper-resistivity with no imposed field. However, a general difficulty with hyperviscosity and hyper-resistivity is that certain aspects of the physics of such systems are significantly modified [32]. It is therefore equally important to assess the features that are likely not to be altered by this manipulation. A detailed discussion of this will be the subject of a forthcoming paper.

Acknowledgments

We thank Tarek Yousef and Eric Blackman for valuable discussions and comments on the manuscript, the Danish Center for Scientific Computing for granting time on the Horseshoe cluster, and the Norwegian High Performance Computing Consortium (NOTUR) for granting time on the parallel computers in Trondheim (Gridur/Embla) and Bergen (Fire).

- R. Beck, A. Brandenburg, D. Moss, A. Shukurov, and D. Sokoloff, Ann. Rev. Astron. Astrophys. 34, 155 (1996).
- [2] S. A. Balbus and J. F. Hawley, Rev. Mod. Phys. 70, 1 (1998).
- [3] D. Biskamp, Magnetohydrodynamic Turbulence. Cambridge: Cambridge University Press (2003).
- [4] J. Cho and E. Vishniac, Astrophys. J. **538**, 217 (2000).
- [5] A. Schekochihin, S. Cowley, G. W. Hammett, J. L. Maron & J. C. McWilliams, New J. Physics 4, 84.1 (2002).
- [6] N. E. L. Haugen, A. Brandenburg, and W. Dobler, Astrophys. J. 597, L141 (2003).
- [7] J. Cho and E. T. Vishniac, Astrophys. J. **539**, 273 (2000).
- [8] J. Maron and P. Goldreich, Astrophys. J. 554, 1175 (2001).
- [9] Cho, J., Lazarian, A., & Vishniac, E., Astrophys. J. 564, 291 (2002).
- [10] Cho, J., Lazarian, A., & Vishniac, E., Astrophys. J. 566, L49 (2002).
- [11] A. Brandenburg, Astrophys. J. **550**, 824 (2001).
- [12] G. Schubert, K. Zhang, M. G. Kivelson, J. D. Anderson, Nature 384, 544 (1996).
- [13] K. K. Khurana, M. G. Kivelson, C. T. Russell, Geophys. Res. Lett. 24, 2391 (1997).
- [14] G. R. Sarson, C. A. Jones, K. Zhang, G. Schubert, Science 276, 1106 (1997).
- [15] E. A. Spiegel and N. O. Weiss, Nature 287, 616 (1980).
- [16] M. Schüssler, (ed. The Hydromagnetics of the Sun), pp. 67. T. D. Guyenne & J. J. Hunt (1984).ESA SP-220
- [17] F. Cattaneo, Astrophys. J. **515**, L39 (1999).
- [18] P. Goldreich and S. Sridhar, Astrophys. J. 438, 763

- (1995).
- [19] N. E. L. Haugen, A. Brandenburg, and W. Dobler, Phys. Rev. E 70, 016308 (2004).
- [20] The Pencil Code is a grid based high order code (sixth order in space and third order in time) for solving the compressible MHD equations; http://www.nordita.dk/data/brandenb/pencil-code.
- [21] D. C. Montgomery, W. H. Matthaeus, L. J. Milano, and P. Dmitruk, Phys. Plasmas 9, 1221 (2002).
- [22] A. Brandenburg and W. H. Matthaeus, Phys. Rev. E, in press (2004); see also astro-ph/0305373.
- [23] R. S. Iroshnikov, Sov. Astron. 7, 566 (1963).
- [24] R. H. Kraichnan, Phys. Fluids 8, 1385 (1965).
- [25] N. Kleeorin and I. Rogachevskii, Phys. Rev. E 50, 2716 (1994).
- [26] A. A. Ruzmaikin and A. M. Shukurov, Astrophys. Spa. Sci. 82, 397 (1982).
- [27] A. Brandenburg, R. L. Jennings, Å. Nordlund, M. Rieutord, R. F. Stein, and I. Tuominen, J. Fluid Mech. 306, 325 (1996).
- [28] P. Goldreich and P. Kumar, Astrophys. J. 363, 694 (1990).
- [29] W.C. Muller, D. Biskamp, and R. Grappin, Phys. Rev. E 67, 066302 (2003).
- [30] U. Schumann, J. Fluid Mech. **74**, 31 (1976).
- [31] Ya. B. Zeldovich, Sov. Phys. JETP 4, 460 (1957).
- [32] A. Brandenburg and G. S. Sarson, Phys. Rev. Lett. 88, 055003 (2002).